International Journal of Solids and Structures 46 (2009) 851–859

Contents lists available at ScienceDirect

International Journal of Solids and Structures

journal homepage: www.elsevier.com/locate/ijsolstr

Stress distribution and wrinkling of webs under non-uniform and asymmetric edge loading

Chung Hwan Kim *

Nano-Mechanical Systems Research Division, Korea Institute of Machinery and Materials, 171 Jang-Dong, Yuseong-Gu, Daejeon 305-343, Republic of Korea

ARTICLE INFO

Article history:
Received 13 May 2008
Received in revised form 18 September 2008
Available online 1 October 2008

Keywords:
Stress distribution
Wrinkling
Web
Non-uniform
Asymmetric
Edge loading

ABSTRACT

Non-uniform edge loading can cause unwanted wrinkling of a web. Here, Airy stress functions are obtained by a modified Fourier series method for webs under non-uniform and different edge loading on each side. The stress distributions of a web under non-uniform edge loading only on one side are subjected to the effect of Saint-Venant's principle. For the web of small aspect ratio under non-uniform edge loading, the stress distribution converges to a uniform distribution or a linear distribution with both the resultant force and the resultant moment being equal to those of the applied loading. Conditions of wrinkling and the corresponding wrinkling modes of a web are found when the edge loadings are different on each side. The non-uniformities and shapes of the applied edge loadings result in different wrinkling conditions. Moreover, the non-uniformities together with the shapes of the applied edge loadings on each side affect the wrinkling conditions.

1. Introduction

Webs of paper, film, sheet metal, and textile are commonly handled not only in many roll-to-roll machineries such as industrial printing machines, roll coaters, and paper making machines but also in many stationary applications such as shadow masks of cathode ray tubes (CRTs), airplane wings, and airbag. The wrinkling as well as the bucking and the vibration of a web in these applications is the main cause of the degradation of the quality of products. Non-uniform edge loading has been known to cause the wrinkling (Lin and Mote, 1996) and buckling (Bert and Devarakonda, 2003; Jana and Bhaskar, 2006; Wang et al., 2008) of a web. When the compressive stress exceeds a critical value associated with the flexural stiffness, wrinkling or buckling of a web occurs. In many studies, the wrinkling of a web has been examined by FEM and analytic methods (Lin and Mote, 1996; Gorman and Singhal, 1993; Timoshenko and Goodier, 1970) and web buckling problems have also been investigated (Bert and Devarakonda, 2003; Jana and Bhaskar, 2006; Wang et al., 2008). In these studies, Airy stress functions were obtained in a closed form for analyzing the wrinkling or buckling of a web under non-uniform and symmetric edge loading along two opposite sides (identical loadings on both sides). However, in general, the shape of the edge loading on one side of a web is likely different from that on the other side, leading to asymmetric edge loading. For example, because the tension distributions of a web transported by rollers are dependent on the pressure distributions at the roller nips and the traction of the rollers, (Benson et al., 1993) the different conditions at each roller could lead to different boundary loadings on each side of the web.

In this paper, Airy stress functions for the stress distributions and the wrinkling modes of a web are calculated under non-uniform and asymmetric loadings (different loadings on each side) by using a modified Fourier series method. In addition,

* Tel.: +82 42 868 7948; fax: +82 42 868 7176.
E-mail address: chkim@kimm.re.kr

0020-7683/$ - see front matter © 2008 Elsevier Ltd. All rights reserved.
doi:10.1016/j.ijsolstr.2008.09.028

the effect of Saint-Venant's principle is examined, and the wrinkling of a web due to the change in the shape of the boundary loading is also studied.

2. Stress distribution due to non-uniform edge loading on one side only

The equation of a plate is given by Eq. (1) (Lin and Mote, 1996; Chia, 1980; Crawford and Atluri, 1975)

$$-T\frac{\partial^2\hat{w}}{\partial\hat{x}^2}-\frac{\partial^2\widehat{F}}{\partial\hat{y}^2}\frac{\partial^2\hat{w}}{\partial\hat{x}^2}+2\frac{\partial^2\widehat{F}}{\partial\hat{x}\partial\hat{y}}\frac{\partial^2\hat{w}}{\partial\hat{x}\partial\hat{y}}-\frac{\partial^2\widehat{F}}{\partial\hat{x}^2}\frac{\partial^2\hat{w}}{\partial\hat{y}^2}+D\nabla^4\hat{w}=0 \tag{1}$$

with the biharmonic equation

$$\nabla^4\widehat{F}=0, \tag{2}$$

where $\hat{w}$ is the transverse displacement, $\widehat{F}$ is the Airy stress function describing non-uniform edge loading, T is uniform tension (per unit width), and $\hat{x}$ and $\hat{y}$ are coordinates. Membrane stiffness is given by $D=Eh^3/[12(1-\nu^2)]$, where E is Young's modulus, h is thickness of the web, and ν is Possion's ratio. In Eq. (1), body force can be neglected because the weight of a very thin web is very small as compared to the tension applied to it. In general, the von Karman plate theory is considered in the case of a large deflection of the plate, that is, $\nabla^4\widehat{F}=Eh[(\partial^2w/\partial x\partial y)^2-(\partial^2w/\partial x^2)(\partial^2w/\partial y^2)]$ (Chia, 1980; Crawford and Atluri, 1975). However, the purpose of this paper is to study the wrinkling mode (eigenvalue problem) and thus, with the assumption of a small deflection of the plate, the linear plate theory is considered, i.e., $\nabla^4\widehat{F}=0$ (Lin and Mote, 1996). The non-uniform edge loading results in non-zero stress distributions inside the plate because $\widehat{F}$ is the function of $\hat{x}$ and $\hat{y}$. Therefore, these stress distributions should be properly determined.

Eqs. (1) and (2) are non-dimensionalized to

$$-w_{,xx}-(T_{xx}w_{,xx}+2T_{xy}w_{,xy}+T_{yy}w_{,yy})+\varepsilon\nabla^4w=0 \tag{3}$$

$$\nabla^4F=0 \tag{4}$$

where $w=\hat{w}/h$, $x=\hat{x}/L$, $y=\hat{y}/L$, L is the length of a web, and the comma denotes partial differentiation. ε is the dimensionless membrane stiffness: $\varepsilon=D/TL^2$. T_{xx} is the normal stress distribution in the x direction, T_{yy} is the normal stress distribution in the y direction, and T_{xy} is the shear stress distribution. These are obtained by $T_{xx}=\partial^2F/\partial y^2$, $T_{xy}=-\partial^2F/\partial x\partial y$, and $T_{yy}=\partial^2F/\partial x^2$, where $F=\widehat{F}/TL^2$.

The prescribed boundary conditions of the stress distributions for the rectangular web under non-uniform normal edge loading on one side only are given by following equations modifying those of Lin and Mote (1996):

$$T_{xx}(0,y)=\sum_{m=1}^{\tilde{m}}\lambda_m\sin\left(\frac{m\pi}{s}y\right) \tag{5}$$

$$T_{yy}(x,0)=T_{yy}(x,s)=0 \tag{6}$$

$$T_{xy}(0,y)=T_{xy}(1,y)=0 \tag{7}$$

$$T_{xy}(x,0)=T_{xy}(x,s)=0 \tag{8}$$

The aspect ratio, s, is defined as B/L, where B and L are the width and length of a web, respectively. λ_m is the amplitude of edge loading, m is an integer, and $\tilde{m}$ is the last integer of the series. Note that the non-zero edge loading is given at edge $x=0$ only, and the edge loading at edge $x=1$, or $T_{xx}(1,y)$, is not specified but to be determined. The edge loading conditions differ from the case of Lin and Mote (1996) where the symmetric edge loading with respect to axis $x=1/2$, or $T_{xx}(0,y)=T_{xx}(1,y)$, is assumed.

The Airy function satisfying the given boundary conditions under symmetric (even) edge loading with respect to axis $y=s/2$ is given by

$$\begin{aligned}F=&\sum_{m=1,3}^{\tilde{m}}\lambda_m\sin\left(\frac{m\pi}{s}y\right)\left[C_{1m}\cosh\left(\frac{m\pi}{s}(x-1)\right)+C_{2m}(x-1)\sinh\left(\frac{m\pi}{s}(x-1)\right)\right]\\&+\sum_{p=1,3}^{\tilde{p}}B_p\sin\left(\frac{p\pi}{2}x\right)\left[D_{1p}\cosh\left(\frac{p\pi}{2}\left(y-\frac{s}{2}\right)\right)+D_{2p}\left(y-\frac{s}{2}\right)\sinh\left(\frac{p\pi}{2}\left(y-\frac{s}{2}\right)\right)\right]\\&+\sum_{q=1,3}^{\tilde{q}}\bar{B}_q\sin\left(\frac{q\pi}{s}y\right)\left[D_{1q}\cosh\left(\frac{q\pi}{s}(x-1)\right)+D_{2q}(x-1)\sinh\left(\frac{q\pi}{s}(x-1)\right)\right]\end{aligned} \tag{9}$$

where

$$C_{1m}=\frac{-\left[\frac{m\pi}{s}\cosh\left(\frac{m\pi}{s}\right)+\sinh\left(\frac{m\pi}{s}\right)\right]}{\left(\frac{m\pi}{s}\right)^2\left[\frac{m\pi}{s}+\cosh\left(\frac{m\pi}{s}\right)\sinh\left(\frac{m\pi}{s}\right)\right]},\quad C_{2m}=\frac{\sinh\left(\frac{m\pi}{s}\right)}{\left(\frac{m\pi}{s}\right)\left[\frac{m\pi}{s}+\cosh\left(\frac{m\pi}{s}\right)\sinh\left(\frac{m\pi}{s}\right)\right]}$$

and

$$D_{1p}=\frac{\frac{s}{2}\sinh\left(\frac{p\pi s}{4}\right)}{\left[\frac{p\pi s}{4}+\sinh\left(\frac{p\pi s}{4}\right)\right]},\quad D_{2p}=\frac{-\cosh\left(\frac{p\pi s}{4}\right)}{\left[\frac{p\pi s}{4}+\sinh\left(\frac{p\pi s}{4}\right)\right]},\quad D_{1q}=\frac{\sinh\left(\frac{q\pi}{s}\right)}{\left[\frac{q\pi}{s}+\sinh\left(\frac{q\pi}{s}\right)\right]},\quad D_{2q}=\frac{-\cosh\left(\frac{q\pi}{s}\right)}{\left[\frac{q\pi}{s}+\sinh\left(\frac{q\pi}{s}\right)\right]}.$$

Each of the three terms in Eq. (9) satisfies the biharmonic equation (Eq. (4)). The first term in Eq. (9) satisfies the normal stress boundary conditions. The second and third terms, satisfying zero normal stress distributions, satisfy the shear boundary conditions when they are added to the first term with properly chosen coefficients B_p and $\overline{B}_q$. Fig. 1(a)–(c) shows the normal stress distributions (T_{xx} and T_{yy}) and the shear stress distribution T_{xy} of the web under the edge loading of $T_{xx}(0,y)=\sin(\pi y/s)$. As shown in these figures, all given boundary conditions are satisfied and the boundary loading on $x=1$, or $T_{xx}(1,y)$, is obtained and observed as the edge loading of large uniform plus small non-uniform perturbation. Although the boundary condition $T_{xx}(1,y)$ is not specified, the boundary loading is appeared due to the effect of the prescribed edge loading of $T_{xx}(0,y)=\sin(\pi y/s)$. The larger the aspect ratio, s, the greater the effects of $T_{xx}(0,y)=\sin(\pi y/s)$. Note that the stress distributions appear to converge to uniform ones as they move farther away from the boundary where the load is applied. Table 1 shows the variation of the largest compressive value of T_{yy} for different $\tilde{p}$ values ($\tilde{p}=\tilde{q}$). As shown in this table, the relative variation between $\tilde{p}=\tilde{q}=5$ and $\tilde{p}=\tilde{q}=101$ is about 1% and the relative variation between $\tilde{p}=\tilde{q}=9$ and $\tilde{p}=\tilde{q}=101$ is below 0.1%. Thus the values of $\tilde{p}$ and $\tilde{q}$ over than 5 can estimate F with a sufficient convergence, however, for the more sufficient convergence, $\tilde{p}=\tilde{q}=31$ is used in this paper.

The Airy function under the anti-symmetric (odd) edge loading with respect to axis $y=s/2$ is also given by a similar form:

$$\begin{aligned}F=&\sum_{m=2,4}^{\tilde{m}}\lambda_m\sin\left(\frac{m\pi}{s}y\right)\left[C_{1m}\cosh\left(\frac{m\pi}{s}(x-1)\right)+C_{2m}(x-1)\sinh\left(\frac{m\pi}{s}(x-1)\right)\right]\\&+\sum_{p=1,3}^{\tilde{p}}\widehat{B}_p\sin\left(\frac{p\pi}{2}x\right)\left[\widehat{D}_{1p}\sinh\left(\frac{p\pi}{2}\left(y-\frac{s}{2}\right)\right)+\widehat{D}_{2p}\left(y-\frac{s}{2}\right)\cosh\left(\frac{p\pi}{2}\left(y-\frac{s}{2}\right)\right)\right]\\&+\sum_{q=2,4}^{\tilde{q}}\overline{B}_q\sin\left(\frac{q\pi}{s}y\right)\left[D_{1q}\cosh\left(\frac{q\pi}{s}(x-1)\right)+D_{2q}(x-1)\sinh\left(\frac{q\pi}{s}(x-1)\right)\right]\end{aligned}\tag{10}$$

where

C_{1m}, C_{2m}, D_{1q}, and D_{2q} are identical to those in Eq. (10). $\widehat{D}_{1p}$ and $\widehat{D}_{2p}$ are given as follows:

$$\widehat{D}_{1p}=\frac{\frac{s}{2}\cosh\left(\frac{p\pi s}{4}\right)}{\left[\frac{p\pi s}{4}+\sinh\left(\frac{p\pi s}{4}\right)\right]},\quad \widehat{D}_{2p}=\frac{-\sinh\left(\frac{p\pi s}{4}\right)}{\left[\frac{p\pi s}{4}+\sinh\left(\frac{p\pi s}{4}\right)\right]}.$$

Fig. 2(a)–(c) shows T_{xx}, T_{yy}, and T_{xy}, respectively, of the web under the edge loading of $T_{xx}(0,y)=\sin(2\pi y/s)$. As shown in these figures, all boundary conditions are satisfied and the boundary loading on $x=1$, or $T_{xx}(1,y)$, is observed as the linearly distributed edge loading. This is also the effect of the loading on $x=0$. Contrary to the case in Fig. 1, non-uniform perturbation is not captured at $x=1$. Note that the stress distributions converge to linear distributions as they move farther away from the boundary where the loading is applied.

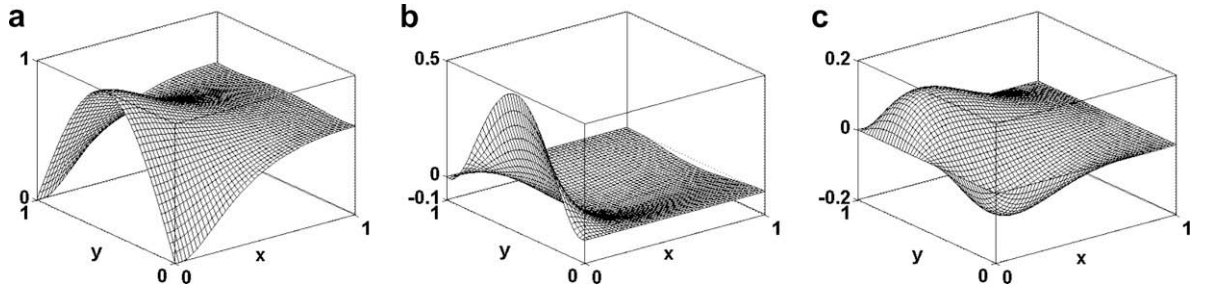

Fig. 1. Stress distributions in the web under edge loading of $T_{xx}(0,y)=\sin(\pi y/s)$ with $s=1$. (a) T_{xx}, (b) T_{yy}, and (c) T_{xy}.

Table 1
Variation of largest compressive value of T_{yy} for different $\tilde{p}$ values ($\tilde{p}=\tilde{q}$).

$\tilde{p}=\tilde{q}$	Largest compressive value of T_{yy}	Variation relative to $\tilde{p}=\tilde{q}=101$(%)
1	0.1831	137.6
5	0.07801	1.22
9	0.07714	0.091
31	0.07707	0
101	0.07707	–

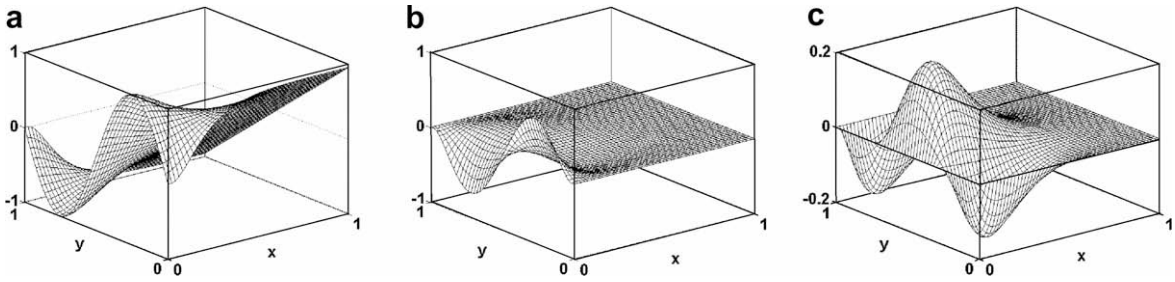

Fig. 2. Stress distributions in the web under edge loading of $T_{xx}(0,y) = \sin(2\pi y/s)$ with $s = 1$. (a) T_{xx}, (b) T_{yy}, and (c) T_{xy}.

3. Effects of Saint-Venant's principle

As discussed in the previous section and shown in Fig. 3, when a symmetric (even) edge loading, such as $\sin(\pi y/s)$, is applied, T_{xx} becomes uniform and converges to the mean value of the applied loading, $\overline{T}_1 = \frac{1}{s}\int_0^s \sin(m\pi y/s)dy = 2/m\pi$ (for example, $\overline{T}_1 = 0.6366$ for $m = 1$), as x increases or in other words, as it moves farther away from the edge. In addition, $\int_0^s T_{xx}(x_1,y)dy = \int_0^s T_{xx}(x_2,y)dy$ = constant holds for two arbitrary values x_1 and x_2, implying that the normal stress in the x direction attains equilibrium at any point in the direction. Thus, the stress distributions and, consequently, their Airy function are physically acceptable and can demonstrate the Saint-Venant's principle.

In the case of an anti-symmetric (odd) loading, for example, $m = 2$, as shown in Fig. 4, T_{xx} becomes linear and converges to $\overline{T}_2 = A\left(y - \frac{s}{2}\right)$, where A makes the resultant moment equal to that of applied one:

$$\sum M = \int_0^s y\sin(m\pi y/s)dy = \int_0^s yA\left(y - \frac{s}{2}\right)dy \tag{11}$$

where $A = -12/m\pi s$. Note that intercept $\overline{T}_2|_{y=0} = 6/m\pi$ is independent of s and becomes 0.9549 for $m = 2$.

For small s (for example, $s \leqslant 0.5$), when a symmetric edge loading is applied, the stress distribution converges to a uniform distribution with the resultant force being equal to that of the applied loading. However, when an anti-symmetric edge

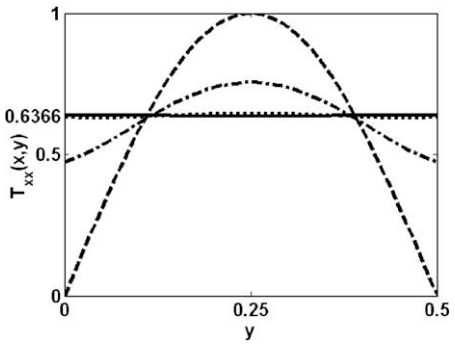

Fig. 3. $T_{xx}(x,y)$ with $m = 1$ and $s = 0.5$ at $x = 0$: ––, $x = 0.25$: – – –, $x = 0.5$:– – –, and $x = 1$: —.

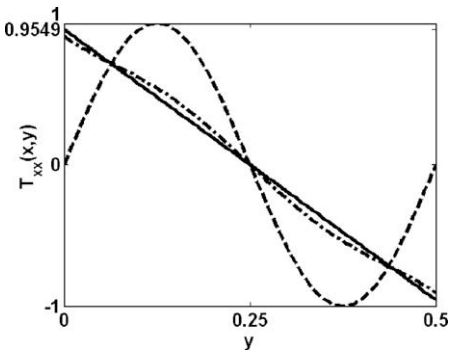

Fig. 4. $T_{xx}(x,y)$ with $m = 2$ and $s = 0.5$ at $x = 0$: ––, $x = 0.25$: – – –, $x = 0.5$: – – –, and $x = 1$: —.

loading is applied, the stress distribution converges to a linear distribution with both the resultant force and the resultant moment being equal to those of the applied loading. In fact, a uniform distribution has a resultant moment equal to zero and so does a symmetric edge loading. Therefore, we can also say that the stress distribution due to a symmetric edge loading converges to a uniform distribution with both the resultant force and the resultant moment being equal to those of the applied loading. Thus, for small, the boundary loading $T_{xx}(1,y)$ can be determined from Eqs. (9) or (10), and we can specify it as a prescribed boundary condition:

$$\overline{T}_{xx}(1,y) = \sum_{m}^{\tilde{m}} \lambda_m \frac{2}{m\pi} \quad \text{for symmetric loading } (m \text{ is odd}) \tag{12a}$$

$$= \sum_{m}^{\tilde{m}} \lambda_m \frac{-12}{m\pi s}\left(y - \frac{s}{2}\right) \quad \text{for anti-symmetric loading } (m \text{ is even}) \tag{12b}$$

4. Wrinkling due to non-uniform edge loading on one side only

Consider again the dimensionless equation of the web under the edge loading of $1 + T_{xx}(0,y)$:

$$-w_{,xx} - (T_{xx}w_{,xx} + 2T_{xy}w_{,xy} + T_{yy}w_{,yy}) + \varepsilon\nabla^4 w = 0 \tag{3}$$

In general, in spite of the non-uniformity of the tension applied (edge loading) along the width of the web, the mean value of the tension applied is maintained by a tension control mechanism. In the work of Lin and Mote (1996), $T_{xx}(0,y) = \lambda\sin(\pi y/s)$ is assumed for the non-uniform component of the edge loading, where the mean value of the edge loading depends on λ. In this paper, however, the non-uniform component of the edge loading is assumed to be $T_{xx}(0,y) = \lambda[\sin(\pi y/s) - 2/\pi]$ in order to guarantee an identical mean value of the tension, regardless of the value of λ, as shown in Fig. 5. The web is under non-uniform loading with $\lambda[\sin(\pi y/s) - 2/\pi]$ in addition to a uniform tension on one side. Thus, the entire edge loading is $1 + \lambda[\sin(\pi y/s) - 2/\pi]$ and the mean value is 1 per unit length in the y direction. This is equivalent, in terms of the resultant magnitude, to the case where a unit mean tension is uniformly distributed along the y direction. From this assumption, we can examine the wrinkling condition of the web with different non-uniformities but the same mean value.

The eigenvalue problem is given by

$$L[w] = \lambda M[w] \tag{13}$$

where $L[] = -\partial^2/\partial x^2 + \varepsilon\nabla^4$ and $M[] = T_{xx}\partial^2/\partial x^2 + 2T_{xy}\partial^2/\partial x\partial y + T_{yy}\partial^2/\partial y^2$. The eigenvalue problem of a web with simply supported boundary conditions is solved by the Rayleigh–Ritz method with the following comparison functions (Lin and Mote, 1996; Meirovitch, 1967):

$$w_{ij} = \sin(i\pi x)\sin(j\pi y/s) \tag{14}$$

where $i,j = 1,2,3,\ldots$

Although, in real applications, two boundaries are simply supported over rollers and are free on the lateral edges, the case where all edges are simply supported is studied for the comparison with the work of Lin and Mote. For $\varepsilon = 10^{-6}$ and $s = 0.5$, the web under non-uniform edge loading applied on one side only has the smallest positive eigenvalue, $\lambda^p_{cr} = 0.2070$, and the largest negative eigenvalue, $\lambda^n_{cr} = -0.2889$ (Case I). When the web is under the same non-uniform edge loadings applied on both sides, the smallest positive and largest negative eigenvalues are found at $\lambda^p_{cr} = 0.1498$ and $\lambda^n_{cr} = -0.2889$, respectively (Case II). In both Case I and Case II, the smallest positive eigenvalues differ from each other, but the largest negative eigenvalues are almost identical. This feature could be explained as follows: wrinkling occurs due to a negative normal stress in the y direction or T_{yy}. In the case of a positive λ, a negative T_{yy} starts at some distance from the edge to the center, as shown in Fig. 6, in which the values of the normal stress distributions in the $y$direction at $y = s/2$ for several different aspect ratios are plotted. Fig. 6 also reveals that as the aspect ratio, s, increases, the negative area of T_{yy} increases and spreads in the opposite

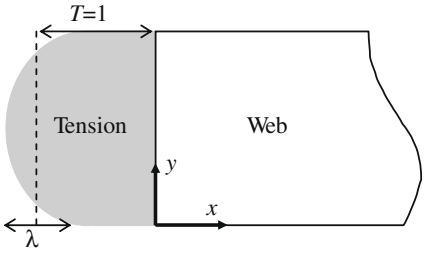

Fig. 5. Web under edge loading of $1 + \lambda[\sin(\pi y/s) - 2/\pi]$ with the mean value of 1 per unit length.

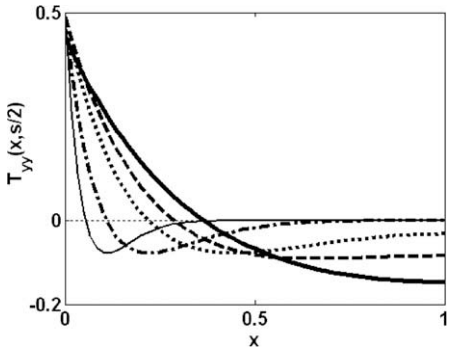

Fig. 6. $T_{yy}(x, s/2)$ for $m = 1$ with different aspect ratios, $s = 2$: ——, $s = 1.5$: – –, $s = 1$: – – – –, $s = 0.5$: – – –, and $s = 0.25$: —.

direction. If an identical edge loading is applied on both sides, there is a larger negative T_{yy} area (in absolute magnitude) in Case II than in Case I because the edge loading applied on one side induces an additional negative T_{yy} on the opposite side of the web. This is more effective in the case of large s (Fig. 6). Thus, a web under two-sided edge loading is wrinkled more easily than that under one-sided edge loading. Consequently, the smallest positive eigenvalue of the former is smaller than that of the latter. When λ is negative, however, a negative T_{yy} starts from the edge and ends in the vicinity of the edge, and the edge loading applied induces negative T_{yy} in the vicinity of the edge only (consider the mirror image of Fig. 6 about the x-axis). Therefore, the edge loading applied on one side does not induce an additional negative T_{yy} on the opposite side of the web, and wrinkling occurs independently in the vicinity of the edge. Accordingly, the largest negative eigenvalues are almost identical in both Case I and Case II.

The wrinkling modes for each eigenvalue are shown more clearly in Figs. 7 and 8. When $\lambda^n_{cr} = -0.2889$, the wrinkling is limited to the vicinity of the edge, but when $\lambda^p_{cr} = 0.2070$, the wrinkling spreads from the edge to the center and then to the other edge. Table 2 shows the variation of λ^p_{cr} and λ^n_{cr} when the number of terms in the comparison functions (i and j of Eq. (14)) increases. ${}^i\lambda_{cr}$ is the value of λ^p_{cr} or λ^n_{cr} when $i(i = j)$ terms are used. As shown in Table 2, λ^p_{cr} converges to 0.2070 rapidly after $i = 18$, but λ^n_{cr} requires more terms to converge. When the convergence criterion is $|({}^{i+1}\lambda_{cr} - {}^{i}\lambda_{cr})/{}^{i+1}\lambda_{cr}| < 0.01\%$,

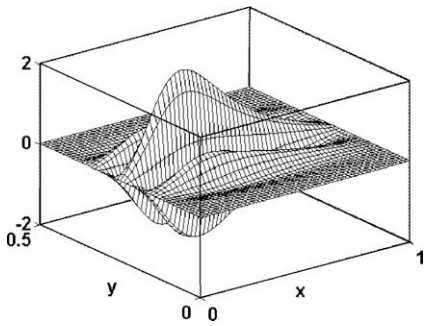

Fig. 7. Wrinkling patterns in a web under edge loading of $T_{xx}(0, y) = \lambda[\sin(\pi y/s) - 2/\pi]$ with $\lambda = \lambda^p_{cr} = 0.2070$.

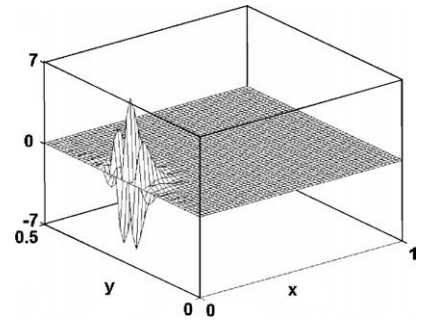

Fig. 8. Wrinkling patterns in a web under edge loading of $T_{xx}(0, y) = \lambda[\sin(\pi y/s) - 2/\pi]$ with $\lambda = \lambda^n_{cr} = -0.2889$.

Table 2
Variation of λ_{cr}^{p} and λ_{cr}^{n} for different number of terms in comparison functions.

$i(i=j)$	λ_{cr}^{p}	$\lvert ({}^{i+1}\lambda_{cr}^{p} - {}^{i}\lambda_{cr}^{p})/{}^{i+1}\lambda_{cr}^{p} \rvert$ (%)	λ_{cr}^{n}	$\lvert ({}^{i+1}\lambda_{cr}^{n} - {}^{i}\lambda_{cr}^{n})/{}^{i+1}\lambda_{cr}^{n} \rvert$ (%)
5	0.6321	56.24	−5.3502	39.73
16	0.2073 (0.20725)	0.232	−0.4684	9.65
17	0.2071 (0.20709)	0.077	−0.4326	8.28
18	0.2070 (0.20704)	0.030	−0.4038	7.13
30	0.2070 (0.20702)	0	−0.2914 (−0.29141)	0.649
31	0.2070 (0.20702)	0	−0.2900 (−0.28995)	0.503
32	0.2070 (0.20702)	0	−0.2889 (−0.28894)	0.350
37	0.2070 (0.20702)	0	−0.2875 (−0.28748)	0.028
38	0.2070 (0.20702)	0	−0.2874 (−0.28743)	0.017
39	0.2070 (0.20702)	0	−0.2874 (−0.28741)	0.007

$\lambda_{cr}^{n} = 0.2874$ $(i = 39)$, but when the convergence criterion is $|{}^{i+1}\lambda_{cr} - {}^{i}\lambda_{cr}|/{}^{i+1}\lambda_{cr}| < 0.5\%$, $\lambda_{cr}^{n} = 0.2889$ $(i = 32)$. The difference between $\lambda_{cr}^{n} = 0.2889$ and $\lambda_{cr}^{n} = 0.2874$ is 0.5% and, based on this convergence study, $i = 32$ can be used with sufficient convergence for the analysis of a wrinkling criteria.

5. Stress distribution due to different non-uniform edge loadings on each side

The Airy function for the stress distribution of a web under the edge loading at $x = 1$ only can be obtained from the mirror images of the Airy functions given by Eqs. (9) and (10):

$$\begin{aligned}\overline{F} = &\sum_{m=1,3}^{\tilde{m}} \lambda_m \sin\left(\frac{m\pi}{s}y\right)\left[C_{1m}\cosh\left(\frac{m\pi}{s}x\right) + C_{2m}x\sinh\left(\frac{m\pi}{s}x\right)\right] \\ &+ \sum_{p=1,3}^{\tilde{p}} B_p \sin\left(\frac{p\pi}{2}(x+1)\right)\left[D_{1p}\cosh\left(\frac{p\pi}{2}\left(y-\frac{s}{2}\right)\right) + D_{2p}\left(y-\frac{s}{2}\right)\sinh\left(\frac{p\pi}{2}\left(y-\frac{s}{2}\right)\right)\right] \\ &+ \sum_{q=1,3}^{\tilde{q}} \overline{B}_q \sin\left(\frac{q\pi}{s}y\right)\left[D_{1q}\cosh\left(\frac{q\pi}{s}x\right) + D_{2q}x\sinh\left(\frac{q\pi}{s}x\right)\right] \end{aligned} \tag{15}$$

The Airy function for an anti-symmetric edge loading with respect to $y = s/2$ is as follows:

$$\begin{aligned}\overline{F} = &\sum_{m=2,4}^{\tilde{m}} \lambda_m \sin\left(\frac{m\pi}{s}y\right)\left[C_{1m}\cosh\left(\frac{m\pi}{s}x\right) + C_{2m}x\sinh\left(\frac{m\pi}{s}x\right)\right] \\ &+ \sum_{p=1,3}^{\tilde{p}} \widehat{B}_p \sin\left(\frac{p\pi}{2}(x+1)\right)\left[\widehat{D}_{1p}\sinh\left(\frac{p\pi}{2}\left(y-\frac{s}{2}\right)\right) + \widehat{D}_{2p}\left(y-\frac{s}{2}\right)\cosh\left(\frac{p\pi}{2}\left(y-\frac{s}{2}\right)\right)\right] \\ &+ \sum_{q=2,4}^{\tilde{q}} \overline{B}_q \sin\left(\frac{q\pi}{s}y\right)\left[D_{1q}\cosh\left(\frac{q\pi}{s}x\right) + D_{2q}x\sinh\left(\frac{q\pi}{s}x\right)\right] \end{aligned} \tag{16}$$

In the case where each side of a rectangular web has different boundary conditions, we can find the stress distributions by superposing the stress distributions from each Airy function satisfying the corresponding boundary conditions. For example, consider a plate with small $s(s = 0.5)$ subjected to an edge loading of $2\lambda_3/3\pi + \lambda_1 \sin(\pi y/s)$ at $x = 0$ and $2\lambda_1/\pi + \lambda_3 \sin(3\pi y/s)$ at $x = 1$, respectively, where $\lambda_1 = \lambda_3 = 1$. The uniform terms $2\lambda_3/3\pi$ and $2\lambda_1/\pi$ are caused by the non-uniform loading on opposite side or $\lambda_3 \sin(3\pi y/s)$ and $\lambda_1 \sin(\pi y/s)$, respectively. In these case, based on Eq. (12a), the boundary conditions of T_{xx} could be specified as follows:

$$T_{xx}(0, y) = 2\lambda_3/3\pi + \lambda_1 \sin(\pi y/s) \tag{17}$$

$$T_{xx}(1, y) = 2\lambda_1/\pi + \lambda_3 \sin(3\pi y/s) \tag{18}$$

The stress distributions are found to be the combination of Airy functions or combinations of Eqs. (9) and (15). T_{xx} is shown in Fig. 9. As shown in the Fig. 9, the boundary conditions are satisfied and uniform offsets at each boundary are found from calculations to be $2\lambda_3/3\pi = 0.2122$ and $2\lambda_1/\pi = 0.6366$.

6. Wrinkling due to different non-uniform edge loadings on each side

Consider a web where the edge loadings of $1 + \lambda_1[\sin(\pi y/s) - 2/\pi]$ and $1 + \lambda_2[\sin(\pi y/s) - 2/\pi]$ are applied on the two opposite sides with different magnitudes of λ_1 and λ_2, as shown in Fig. 10. Note that the resultant mean tensions at each side are identical, that is, 1 per unit length.

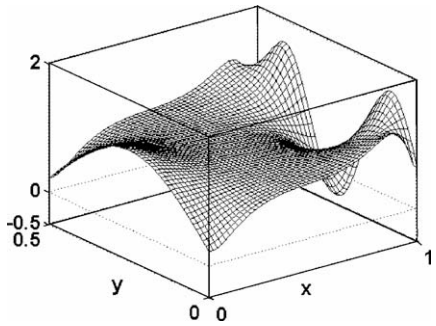

Fig. 9. T_{xx} of a web under edge loading of $T_{xx}(0,y) = 2\lambda_3/3\pi + \lambda_1 \sin(\pi y/s)$ and $T_{xx}(1,y) = 2\lambda_1/\pi + \lambda_3 \sin(3\pi y/s)$, where $\lambda_1 = \lambda_3 = 1$.

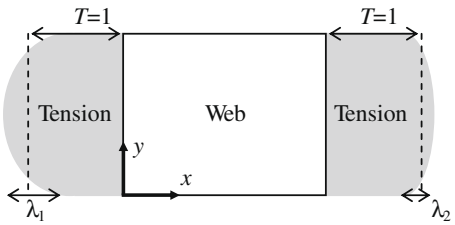

Fig. 10. Web under edge loadings of $1 + \lambda_1[\sin(\pi y/s) - 2/\pi]$ and $1 + \lambda_2[\sin(\pi y/s) - 2/\pi]$ on two opposite sides with different magnitudes of λ_1 and λ_2.

The eigenvalues of the web with $s = 0.5$, $\varepsilon = 10^{-6}$, and $\lambda_1 = 0$ are found to be $\lambda^p_{2cr} = 0.2070$ and $\lambda^n_{2cr} = -0.2889$, and the values of λ_{2cr} depending on λ_1 are plotted in Fig. 11. In this analysis, $i = j = 32$ is also used as the number of terms of the comparison functions. If λ_1 is larger than $\lambda^p_{1cr} = 0.2070$ or smaller than $\lambda^n_{1cr} = -0.2889$, then λ^p_{2cr} and λ^n_{2cr} are trivial solutions. In the region of non-trivial solutions, the negative eigenvalue λ^n_{2cr} is almost constant. The positive eigenvalue λ^p_{2cr} decreases with a gentle slope in the case of a negative λ_1; however, it decreases rapidly with λ_1, in the case of a positive λ_1. In other words, if an additional edge loading with a convex center acts on the opposite side, the web with the convex center is wrinkled more easily than that with the concave center. On the contrary, the additional edge loading with a concave center acting on the opposite side does not significantly affect the condition of wrinkling, irrespective of the shape of the existing edge loading. Because the edge loading with a convex center induces a negative normal stress in the width direction (negative T_{yy}), spreading over the large area of the web, the additional edge loading on the opposite side with a convex center adds a negative T_{yy} to the existing negative T_{yy}, causing wrinkling to occur more easily.

7. Conclusions

In this study, the general form of the Airy stress function of a web under non-uniform and different edge loadings on each side from one another is obtained using a modified Fourier series method. The stress distributions of the web under a non-uniform edge loading on one side only are calculated, and the corresponding Airy function is found to verify the effect of Saint-Venant's principle. For a small aspect ratio, when an arbitrary non-uniform edge loading is applied, the stress distri-

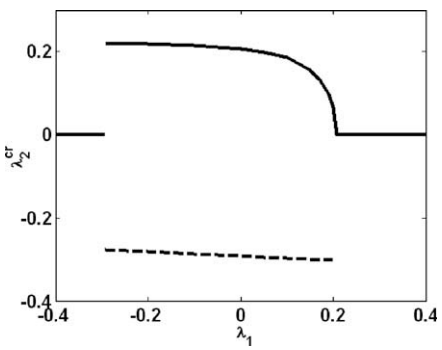

Fig. 11. Values of λ_{2cr} depending on λ_1, λ^p_{2cr}: —, λ^n_{2cr}: ---.

bution converges to a uniform distribution or a linear distribution with an equal resultant force and moment. For a large aspect ratio, however, the boundary loading is not completely equalized at the opposite boundary and consequently, the stress distribution approaches a uniform (not exactly uniform) one or a linear (not exactly linear) one. When the web is under a non-uniform edge loading, the smallest positive degree of non-uniformity (ratio of the amplitudes between that of non-uniform loading and that of uniform loading) that initiates the wrinkling is significantly affected by the edge loading on the opposite side. However, the largest negative degree of non-uniformity is not affected considerably by the edge loading on the opposite side. An additional edge loading with a convex center applied on the opposite side wrinkles the web with the convex center more easily than that with the concave center.

When a web is only under non-uniform loading without uniform tension, Eq. (3) becomes

$$-(T_{xx}w_{,xx} + 2T_{xy}w_{,xy} + T_{yy}w_{,yy}) + \varepsilon\nabla^4 w = 0 \tag{19}$$

Because T_{xx}, T_{xy}, and T_{yy} are functions of λ_m, the value of λ_m is associated with the buckling coefficient. Further study on the buckling problem of webs under non-uniform and asymmetric edge loadings could be dealt with as another issue.

References

Benson, R.C., Chiu, H.C., LaFleche, J., Stack, K.D., 1993. Simulation of wrinkling patterns in webs due to non-uniform transport conditions. In: Proceedings of the 2nd International Conference on Web Handling, pp. 333–347.

Bert, C.W., Devarakonda, K.K., 2003. Buckling of rectangular plates subjected to nonlinearly distributed in-plane loading. International Journal of Solids and Structures 40, 4097–4106.

Chia, C.Y., 1980. Nonlinear Analysis of Plates. McGraw-Hill, Inc..

Crawford, J., Atluri, S., 1975. Non-linear vibrations of a flat plate with initial stresses. Journal of Sound and Vibration 43 (1), 117–129.

Gorman, D.J., Singhal, R.K., 1993. A superposition-Rayleigh–Ritz method for free vibration analysis of non-uniformly tensioned membranes. Journal of Sound and Vibration 162, 489–501.

Jana, P., Bhaskar, K., 2006. Stability analysis of simply-supported rectangular plates under non-uniform uniaxial compression using rigorous and approximate plane stress solutions. Thin-Walled Structures 44, 507–516.

Lin, C.C., Mote Jr., C.D., 1996. Eigenvalue solutions predicting the wrinkling of rectangular webs under non-linearly distributed edge loading. Journal of Sound and Vibration 197, 179–189.

Meirovitch, L., 1967. Analytic Methods in Vibrations. Macmillan Publishing Co., Inc..

Timoshenko, S.P., Goodier, J.N., 1970. Theory of Elasticity, third ed. McGraw-Hill.

Wang, X., Gan, L., Zhang, Y., 2008. Differential quadrature analysis of the buckling of thin rectangular plates with cosine-distributed compressive loads on two opposite sides. Advances in Engineering Software 39, 497–504.